

# Three-Dimensional Computations of Ingress in Gas Turbine Cooling Systems

Paul Lewis<sup>1</sup> and Michael Wilson<sup>2</sup>

<sup>1</sup> Department of Mechanical Engineering, University of Bath

<sup>2</sup> Department of Mechanical Engineering  
University of Bath

Claverton Down, Bath BA2 3BA, United Kingdom

Phone: +44-1225-386325, FAX: +44-1225-386928, E-mail: m.wilson@bath.ac.uk

## ABSTRACT

This paper describes a computational study of ingress in a simplified model of a gas-turbine rotor-stator wheel-space with an axial clearance rim seal, with non-axisymmetric flow conditions created using a stator vane in an external mainstream. Steady-state computational fluid dynamics (CFD) simulations are carried out using the commercial CFD code CFX in order to investigate the effects of geometry and boundary condition assumptions on the results, providing information for the design of simplified experimental apparatus. The computations are carried out for a rotational Reynolds number of  $2.5 \times 10^6$ , such as might typically be used in experiments, and for non-dimensional values of mainstream and sealing flow-rates selected to match some of the conditions that might be encountered in engines.

The computed results show that the amount of ingress into the wheel-space depends upon the distance between the stator vane trailing edge and the rim seal. A recirculation region set up within the seal is responsible for transporting ingested fluid inwards into the wheel-space at some circumferential locations and for sealing the wheel-space from this ingress at others.

The sealing effectiveness of the rim seal is calculated from computed levels of concentration of a tracer scalar variable. The concentration results illustrate the importance of three dimensional effects, and computed heat transfer results show that frictional heating due to the rotating disc needs to be considered in planning experiments to investigate ingress phenomena further.

## NOMENCLATURE

a	wheel-space inner radius [m]
b	wheel-space outer radius [m]
C	concentration of scalar quantity
$C_p$	pressure coefficient (Eq. 3)
$C_w$	non-dimensional sealing flow rate ( $=\dot{m}_s / \mu b$ )
$C_{w,MIN}$	minimum $C_w$ required to prevent ingress (Eq. 1)
G	wheel-space gap ratio ( $=s/b$ )
$G_c$	seal gap ratio ( $=s_c/b$ )
$\dot{m}$	mass flow rate [kg/s]
p	static pressure [Pa]
r, $\phi$ , z	radial, circumferential and axial coordinates
$Re_\phi$	rotational Reynolds number (Eq. 2a)
$Re_z$	mainstream flow axial Reynolds number (Eq. 2b)
s	wheel-space rotor-stator axial separation [m]

$s_c$	axial seal clearance [m]
T, $T_o$	static temperature, total temperature [K]
$\bar{T}$	non-dimensional static temperature (Eq. 6)
v	velocity [m/s]
$\bar{v}_r$	average radial velocity in the seal (Eq. 4)
x	non-dimensional radius ( $=r/b$ )
$y^+$	wall-distance Reynolds number
$\beta$	swirl ratio ( $=v_\phi/\Omega r$ )
$\phi_b$	vane spacing angle [degrees]
$\eta$	sealing effectiveness (Eq. 5)
$\mu$	dynamic viscosity [kg/m/s]
$\theta$	non-dimensional angle ( $=\phi/\phi_b$ )
$\rho$	density [kg/m <sup>3</sup> ]
$\Omega$	disc rotation rate [rad/s]

## Subscripts

r, $\phi$ , z	radial, circumferential or axial component
e	external (mainstream), at mainstream inlet
i	internal (wheel-space)
s	at sealing flow inlet

## INTRODUCTION

The internal air system in a gas-turbine engine is of great importance in providing cooling air to temperature-critical components such as the turbine blades, and also pressurises the seals to prevent ingestion of hot gases from the mainstream into the wheel-spaces between rotating and stationary elements. Minimising this ingestion, or ingress, is particularly important in the high pressure turbine stages immediately downstream of the combustion chamber, where the high temperature of ingested mainstream gas can lead to fatigue and damage in the important region around the outer rim seal, including possibly the blade-cooling air receiver holes located near the periphery of the turbine disc.

The rotating flow between a rotating turbine disc (the rotor) and an adjacent stationary casing (the stator) creates a radial pressure gradient that encourages ingestion (radially inward flow) of mainstream gas, as illustrated schematically in Fig. 1. The stationary vanes and rotating blades in the turbine annulus create non-axisymmetric, unsteady variations of pressure that also drives hot gas into the wheel-space in regions of high external pressure. The relative importance of the influence on ingress of the flow inside the wheel-space, the stationary vanes and the rotating blades has been studied using simplified experimental rotating-disc rigs, where greater control can be exerted and more detailed measurements can be made than is usually the case with instrumented engine components. A summary of such research has been given by Owen (2006).

Bayley and Owen (1970) carried out experiments for so-called “rotationally-induced” ingestion into an unconfined simple rotor-stator system with an axial clearance rim-seal, and using a theoretical “orifice model” for the seal correlated the minimum non-dimensional flow rate of sealing air,  $C_{W,MIN}$  ( $= \dot{m}_s / \mu b$ ), required to prevent ingress by the expression:

$$C_{W,MIN} = \Phi_{MIN} \times G_C \times Re_\phi, \text{ where } \Phi_{MIN} = 0.61 \quad (1)$$

(where  $G_C$  is the non-dimensional axial width of the seal and  $Re_\phi$  is the rotational Reynolds number based on the disc outer radius,  $b$ ). Graber et al. (1987) made measurements of ingestion of carbon dioxide into a rotor-stator wheel-space from a swirling external mainstream flow for a number of different seal geometries. The results were in reasonable agreement with Eq. (1), although  $\Phi_{MIN}$  was found not to be constant but to decrease with increasing  $Re_\phi$ .

Phadke and Owen (1988a,b,c) found that, for “externally-induced” ingestion due to a non-axisymmetric external flow,  $C_{W,MIN}$  was independent of  $Re_\phi$  and increased with increasing axial Reynolds number,  $Re_Z$ , for the external flow. Phadke and Owen and others have correlated both  $C_{W,MIN}$  and  $\eta$ , the non-dimensional sealing effectiveness based on local concentration of fluid from the external flow, with a non-dimensional measure of the peak pressure difference in the external flow.

A review of research carried out under engine-relevant mainstream conditions involving rotating blades as well as stationary vanes is given by Owen (2006). Wang et al (2007) discuss results of unsteady computations and comparisons with experiments for different combinations of locations for the stator vanes, the axial clearance seal and the rotor blades. The pressure field due to the rotor blades was found to dominate ingestion for the closely-spaced stages considered. Roy et al (2007) computed velocity distributions and measured sealing effectiveness for a radial clearance rim seal, and found that large-scale unsteady flow structures could occur within the wheel-space (other similar findings to this are also reported by Owen, 2006).

Correlations such as that given in Eq. (1) based on the results of very much simplified experiments have been used by designers to estimate the amount of sealing flow needed in engines. Better theoretical models of ingress and improved versions of design correlations are likely to result from the further investigation of the individual contributions to ingress of the fluid dynamics of the wheel-space, the non-axisymmetric external flow produced by the stationary vanes and the additional unsteady variations due to rotating turbine blades. The present paper describes a computational study of the first two of these influences. A simplified rotor-stator system is modelled and a stator vane is used to produce a representative pressure field in the external mainstream. Computations are carried out, assuming steady flow in the absence of rotating blades, at conditions relevant to the experimental rigs that are used to provide understanding and detailed quantitative information on some of the fundamental features of ingress. The results are intended to be used to guide aspects of the design of new apparatus.

### COMPUTATIONAL DOMAIN AND MODEL

The computational domain, illustrated in Fig. 1, comprises a rotor-stator wheel-space having an outer radius  $b = 0.216\text{m}$  and an axial-clearance rotor-side rim seal leading to an outer annulus representing the mainstream gas path through the turbine stage. The annulus height is  $10\text{mm}$  and the wheel-space gap ratio and seal gap ratio are  $G = 0.07$  and  $G_C = 0.01$  respectively. The radial offset to the annulus boundary surface on the stator side was included as a result of preliminary computations that showed that the mainstream flow could stagnate otherwise at the top of the seal on the rotor side, leading to very low computed levels of ingress. This may be desirable in practice, however experimental apparatus would be likely to be designed to promote ingress at the chosen flow conditions for the purpose of making accurate and informative measurements.

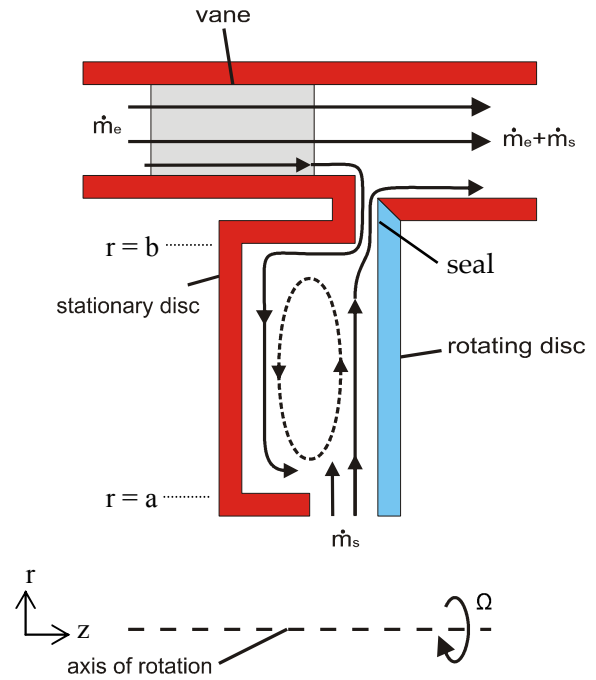


Fig. 1 Schematic of configuration studied computationally

A stator vane of generic geometry is included in the mainstream annulus upstream of the seal, see Fig. 2, to provide circumferential variations of pressure and velocity. A  $15^\circ$  circumferential sector has been modelled computationally, representing the pitch between each of twenty four stator vanes proposed for a future experimental rig. Two geometric configurations have been tested, having different axial spacings of  $7.92\text{mm}$  and  $15.42\text{mm}$  between the vane trailing edge and the seal. These are denoted here as NEAR-VANE and FAR-VANE configurations respectively.

The system has two inlets; the sealing air inlet at the inner radius of the wheel-space (at  $r = a$ , see Fig. 1) and the external mainstream inlet upstream of the vane, at both of which uniform values for velocity components and temperature are prescribed as described below. An average static pressure is prescribed at the mainstream outlet boundary. Cyclic symmetry and no-slip conditions are applied at other boundaries as appropriate and all solid boundary surfaces are assumed to be adiabatic.

An unstructured mesh has been used, with a blend of quadrilateral elements near wall surfaces and a Delaunay triangulation in the core away from them, rotated around the central axis. The mesh around the stator vane was generated using regular layers in the near wall region and an advancing front scheme in the core. Sensitivity to mesh size was tested over a wide range, see Table 1.

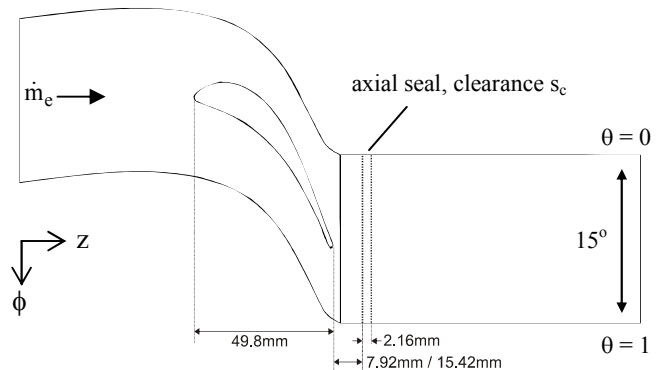


Fig. 2 Geometric arrangement for mainstream and stator vane (cyclic symmetry imposed at boundaries at  $\theta = 0$  and  $\theta = 1$ )

Table 1 Computational grid sizes studied

Geometry	Mesh	Elements		
		Total	Circumferential	Axial (Across Seal Gap)
NEAR-VANE	Coarse	583,200	45	15
	Regular	1,526,220	90	25
	Fine	2,777,355	135	33
	Very Fine	3,963,600	180	39
	Very Fine (90)	1,993,140	90	39
FAR-VANE	Regular	1,579,140	90	25

As illustrated in red in Fig. 1, all of the wall boundary surfaces are stationary with the exception of the rotor. Other computations were carried out for which the annulus inner boundary surface attached to the rotor also rotated. In this case, it was found that Taylor vortices were set up in the mainstream flow downstream of the seal. These vortices affected the computed flow structure in the seal and initiated unsteady flow inside the wheel-space (related possibly to structures described by Roy et al (2007) and Owen, 2006). These destabilising effects are still being studied and are not considered in detail here, as the single blade pitch angular domain shown in Fig. 2 was found to constrain the flow to remain steady under the assumption of cyclic symmetry.

The commercial code ANSYS-CFX Version 10 was used for the computations. This finite volume algebraic multi-grid solver uses a pressure coupling method for the non-staggered mesh based on that of Rhie and Chow (1982). The advection scheme is second order accurate, based on the method of Barth and Jespersen (1989). In addition to the RANS momentum and energy equations, a further transport equation was solved for conservation of a non-interacting scalar. This allowed a tracer to be introduced at the external mainstream inlet in order to calculate the amount of ingress and hence sealing effectiveness. Gravitational buoyancy effects were ignored. Normalised convergence levels below  $10^{-5}$  were achieved.

The Baseline (BSL) turbulence model of Menter (1994) employed is a blended formulation of a  $k-\omega$  model in the near wall region and a  $k-\epsilon$  model further from the wall. So-called “scaleable” wall functions allow near wall grid resolution of  $y^+ \approx 11$ . A similar computational approach was taken by Wang et al (2007). The CFX code was validated by Lewis et al (2007) using the same turbulence model for a rotor-stator system with a superposed flow, and very similar methods and software have been used by, for example, Jarzombek et al (2007) to study gas-turbine cooling systems and by Sun et al (2006) to compute the unstable flows inside rotating cavities.

### GOVERNING PARAMETERS AND TEST CONDITIONS

The rotational Reynolds number for the wheel-space is:

$$Re_\phi = \frac{\rho\Omega b^2}{\mu} \quad (2a)$$

and the mainstream annulus axial Reynolds number is:

$$Re_z = \frac{\rho v_{z,e} b}{\mu} \quad (2b)$$

The values of the main parameters used for the computations are:

$$\begin{aligned} \Omega &= 848 \text{ rad/s } (\approx 8,000 \text{ rpm}) \\ C_w &= 1,600 \end{aligned}$$

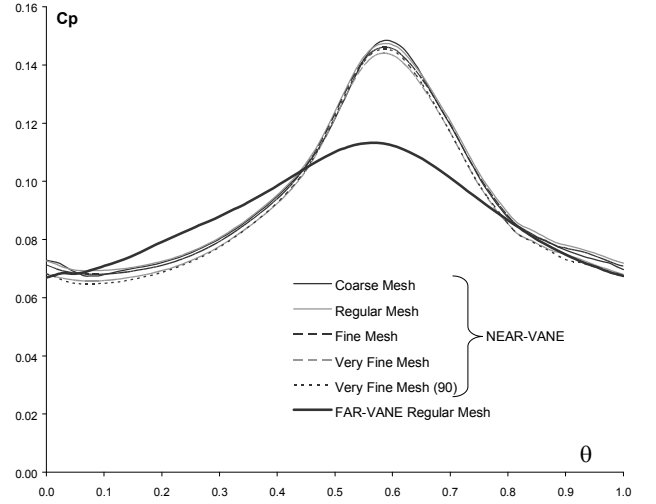


Fig. 3 Computed circumferential static pressure distributions in the mainstream radially outward of the seal

$$\begin{aligned} v_{z,e} &= 196 \text{ m/s} \\ Re_\phi &= 2.5 \times 10^6 \\ Re_z &= 2.7 \times 10^6 \end{aligned}$$

The stator vane used gives an average flow angle of around  $24^\circ$  to the circumferential in the mainstream in the region radially outward of the seal. The values of  $\Omega$  and  $C_w$  were selected as likely test conditions in planned future experiments, and the value of  $Re_z$  used is that which gives rise to a swirl ratio  $\beta_e \approx 1$  in the mainstream at the seal location (matching qualitatively conditions in the experiments by Graber et al, 1987). The sealing flow rate used is much lower than the value  $C_{w,MIN} = 15,250$  suggested by Eq. (1) for this configuration. The matching of the sealing flow rate to the rotational speed through the non-dimensional parameters  $Re_\phi$  and  $C_w$  allow the findings for fluid dynamics to be extrapolated with some confidence to the engine situation, see Owen and Rogers, 1989.

### FLUID DYNAMICS RESULTS

The circumferentially varying pressure field in the external mainstream produced by the stationary vane is illustrated in Fig. 3. The pressure coefficient,  $C_p$ , is based on  $p_e$ , the computed external mainstream static pressure at the half height of the annulus radially outward of the seal, and  $\bar{p}_i$ , the spatially averaged static pressure on the stator inside the wheel-space at a non-dimensional radial location  $x = 0.95$ , and is defined as follows:

$$C_p = \frac{p_e - \bar{p}_i}{0.5\rho\Omega^2 b^2} \quad (3)$$

The circumferential distribution for  $C_p$  for the NEAR-VANE configuration shown in Fig. 3 shows a minimum at a non-dimensional circumferential location  $\theta \approx 0.07$  and a distinct peak at  $\theta \approx 0.61$ .

The circumferential variation of  $C_p$  decreases with increasing distance downstream from the vane trailing edge. With the seal in the further downstream (FAR-VANE) position the peak magnitude for  $C_p$  is approximately half that for the NEAR-VANE configuration, due to mixing and pressure recovery in the mainstream. (In an engine, changing the seal location relative to the vane trailing edge in this way would increase the relative effect on ingress of the pressure distribution due to the rotating turbine blades.) The mainstream pressure variations for the FAR-VANE configuration were found to give rise to very low levels of ingress, and further results are presented here only for the NEAR-VANE configuration.

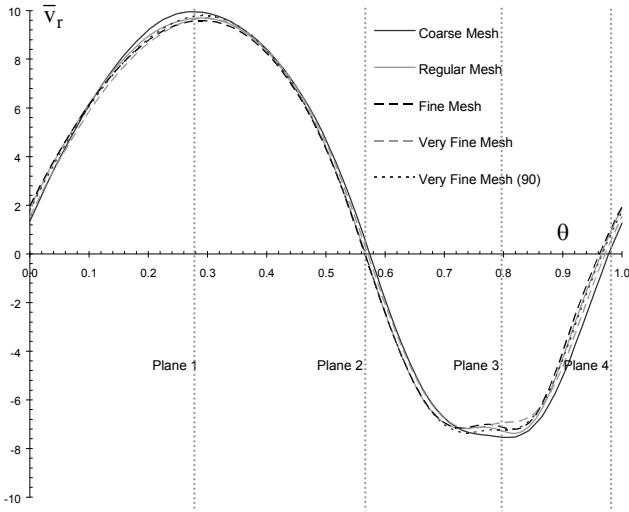


Fig. 4 Computed circumferential variation of average radial velocity within the seal

The influence of the mainstream pressure variations in driving fluid into the wheel-space can be characterised using  $\bar{v}_r$ , a mass-weighted average radial velocity across the seal, defined as:

$$\bar{v}_r = \frac{\int_{s_c} v_r (\rho v_r) dz}{\int_{s_c} (\rho v_r) dz} \quad (4)$$

The circumferential variation of  $\bar{v}_r$  at the seal half-height ( $x \approx 1.01$ ) is shown in Fig. 4. The distribution shows a peak negative value (indicating net flow radially inward) at non-dimensional circumferential position  $\theta \approx 0.73$ , a location shifted circumferentially by about one-eighth of the stator-vane pitch in the direction of rotation of the disc from that ( $\theta \approx 0.61$ ) shown in Fig.3 for the corresponding maximum driving pressure. This illustrates the effect of the tangential swirl in the mainstream flow on the flow within the seal.

The velocity vectors shown in Fig. 5 illustrate the secondary flow (i.e. the flow in the axial-radial plane) in the seal at the four circumferential planes indicated in Fig. 4. In Plane 1, where  $\bar{v}_r$  is a maximum, this radially outward flow is due to the boundary layer on the rotor. In Plane 2, where  $\bar{v}_r \approx 0$ , the secondary flow velocity magnitude is small in the seal region, with some outward flow on the rotor side and some flow drawn inwards from the mainstream onto the stator side of the seal. Ingress into the system is a maximum at Plane 3, where a powerful recirculation is formed at the stator side of the seal. This recirculation transports the fluid ingested into the seal from the mainstream further radially inward and this fluid then flows towards the stator as it enters the wheel-space.

In Plane 4, where again  $\bar{v}_r \approx 0$ , the strong recirculation apparent at Plane 3 is maintained, but now acts to seal the system. This is due to the smaller pressure differences between the wheel-space and the mainstream influencing the flow at this location ( $\theta \approx 1$ ), see Fig. 3. Similar underlying flow structures to those described here are expected also to be found in engines, modified by additional unsteady pressure variations due the rotating turbine blades.

### COMPUTED SEALING EFFECTIVENESS

The sealing effectiveness of the system,  $\eta$ , is evaluated using the computed local concentration (mass-fraction)  $C$  of the non-participating scalar “tracer” variable transported throughout the system:

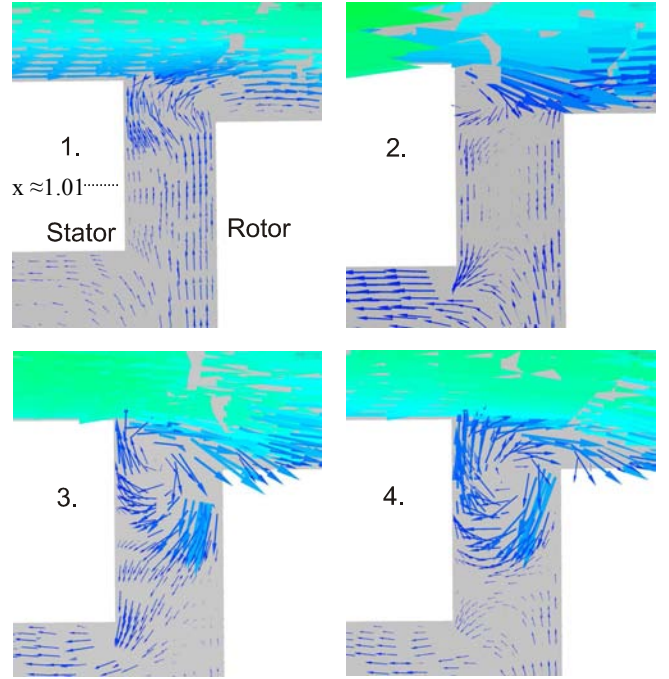


Fig. 5 Secondary flow in the seal at the four circumferential planes defined in Fig. 4

$$\eta = 1 - \frac{C - C_s}{C_e - C_s} \quad (5)$$

where  $C_s$  and  $C_e$  are the prescribed values of concentration at the sealing and mainstream inlets respectively. (If no ingestion occurs,  $C = C_s$  inside the wheel-space and the sealing effectiveness is unity.)

Values for sealing effectiveness are shown in Fig. 6a and Fig. 6b for near-wall solution points adjacent to the stator and rotor respectively, point results having been averaged circumferentially to give these radial distributions. The results show significant grid sensitivity, particularly for the coarser grids. There are no similarly significant differences for the computed velocity field (see Fig. 4), suggesting that the computed transport of the scalar variable is more sensitive to the grid than are the associated velocities.

Fig. 6a shows that (on each of the different meshes tested) the computed sealing effectiveness is approximately constant with radius near the stator. This behaviour is consistent with ingested mainstream flow flowing radially inward in the wheel-space within the boundary layer on the stator. The ingested fluid then migrates axially across the wheel-space towards the rotor, however there is no entrainment of fresh fluid into the stator boundary layer to dilute the concentration. (The spatially averaged computed flowfield within the wheel-space was found to be very similar to that in a classical rotor-stator system with a superposed radial outflow, where for the value of gap ratio  $G$  considered here there are boundary layers on the rotor and stator separated by a rotating core of fluid, see Owen and Rogers, 1989.)

The radial variation of averaged effectiveness with radial location near the rotor is more significant than for the stator. At the inner radius ( $r = a$  corresponding to  $x = 0.61$  for the configuration considered) where sealing flow enters the system, effectiveness approaches unity. As radius increases, fluid is entrained into the rotor boundary layer from the stator, increasing the concentration of ingested fluid and thus reducing the effectiveness.

A qualitative comparison is made in Fig. 6a between the computed values for sealing effectiveness near the stator and local values measured on the stator in experiments Roy et al (2007), for a

similar value of non-dimensional sealing flow-rate  $C_w$  although at lower values of  $Re_\phi$  and  $Re_z$ . The lower values of effectiveness measured by Roy et al for  $x > 0.8$  (the outer region of the wheel-space closest to the seal) suggests that more ingress occurred in this experiment than in the computations described here. As mentioned above, other computations were carried out for which there was greater non-uniformity in the mainstream flow downstream of the seal that gave rise to more complex flow inside the wheel-space. The computed values of effectiveness in this case were lower than those shown in Fig. 6a, suggesting that the greater mainstream non-uniformity in this case may have had some similar effects to those due to the rotating blades used on the rig of Roy et al.

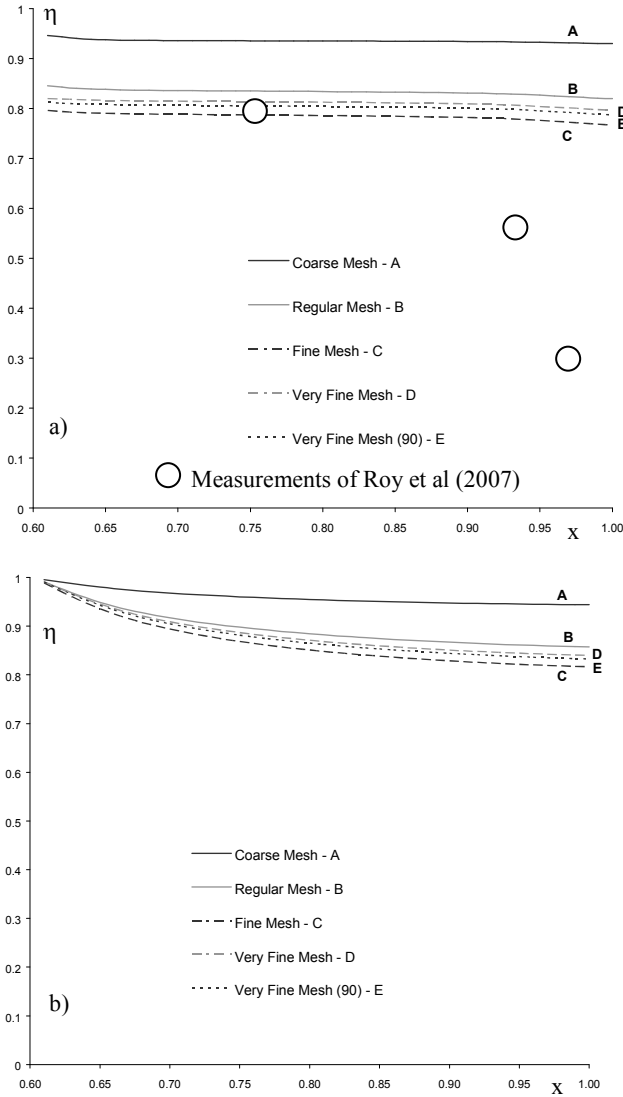


Fig. 6 Computed averaged values of effectiveness: (a) near the stator, (b) near the rotor

### COMPUTED TEMPERATURE DISTRIBUTIONS

The inlet total temperature of the wheel-space sealing flow was set at  $T_{o,s} = 20^\circ\text{C}$  for the computations and that of the mainstream flow at inlet at  $T_{o,e} = 60^\circ\text{C}$ . These values were based on the conditions in heat transfer experiments by Lewis et al (2007) for a different turbine cooling application.

Fig. 7 shows computed, circumferentially averaged, profiles of non-dimensional static temperature  $\bar{T}$  on the stator and rotor, where  $\bar{T}$  is defined here as:

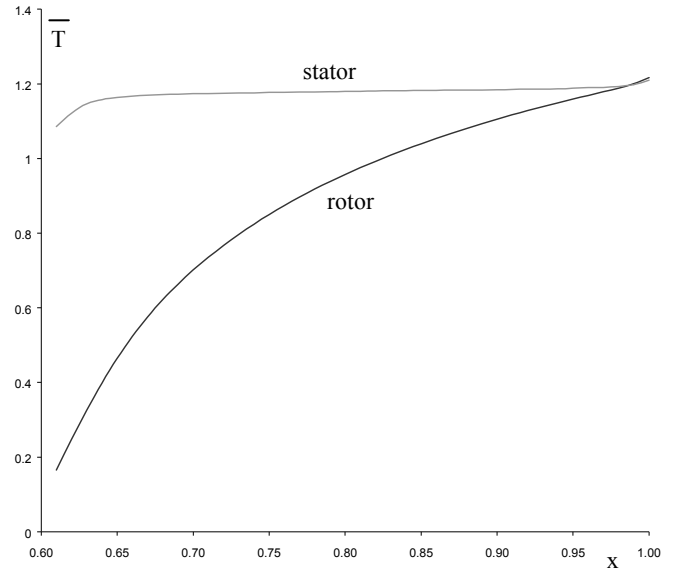


Fig. 7 Computed circumferentially averaged values of non-dimensional temperature  $\bar{T}$  on the rotor and stator

$$\bar{T} = \frac{T - T_{o,s}}{T_{o,e} - T_{o,s}} \quad (6)$$

Two mechanisms contribute to the elevated temperatures computed within the wheel-space; the ingress of higher temperature fluid from the mainstream and frictional heating (windage) due to the rotating disc.

Fig. 7 shows that dimensionless temperatures reach values greater than unity at both the rotor and stator surfaces, indicating that for this situation the fluid in the wheel-space is heated above that of the external mainstream. This is caused by frictional heating, exaggerated by the use of adiabatic boundary conditions at solid surfaces and the low value of sealing flow rate used. Typically in engines  $(T_e - T_s) \approx 1000\text{K}$  and the windage heating may be up to around 50K, however the values used in the computations are characteristic of test conditions that might be used in simplified experiments. Sealing effectiveness can be defined in terms of  $\bar{T}$  rather than local concentration as in Eq. (5), and the results shown in Fig. 7 are a caution to researchers designing experiments to study the thermal effects of ingress using modest differences in temperature, in order for example to make heat transfer measurements using thermochromic liquid crystal (TLC), as it is necessary to account for both ingestion and windage. Such experiments are currently being devised by colleagues of the authors, based on further development of the TLC techniques described by Lock et al (2005). Computations such as those described here, as well as measurements of concentration, are likely to be needed in order to interpret fully measurements of temperature and heat transfer.

### CONCLUSIONS

Three-dimensional steady turbulent flow computations of a rotor-stator system and an external mainstream have been carried out using the commercial CFD code CFX, at conditions typical of those likely to be used in simplified experiments devised to monitor and measure the effects of ingress of hot fluid from the mainstream into the rotor-stator wheel-space.

The computed results show that a stator vane in the mainstream, with its trailing edge sufficiently close to the rotor-stator axial seal, produces a non-axisymmetric flow distribution sufficient to cause significant levels of ingress into the wheel-space, as deduced from sealing effectiveness values calculated using computed concentrations of a tracer scalar variable. Investigation of the fluid dynamics within the axial clearance seal shows that ingested fluid is trans-

ported radially inwards, and towards the stator boundary layer inside the wheel-space, through the action of a recirculating flow established in the seal which also acts to seal the system locally from ingress at other circumferential locations, even when the superposed wheel-space sealing flow rate is low compared with the minimum expected theoretically to be required to prevent ingress.

Greater grid sensitivity was observed for computed results for effectiveness compared with velocity distributions. Computations of the thermal field suggest that identification of the thermal effects of ingress in simplified experiments may be complicated by the frictional heating (windage) of the fluid in the wheel-space due to the rotating disc.

#### ACKNOWLEDGEMENTS

Mr Lewis is a PhD student supported by a studentship from the Engineering Innovative Manufacturing Research Centre at Bath, which is funded by the UK Engineering and Physical Sciences Research Council. The present research into ingress in gas turbines has been stimulated and supported by collaboration with Mitsubishi Heavy Industries, Japan.

#### REFERENCES

- Barth, T. J., and Jespersen, D. C., 1989. The design and application of upwind schemes on unstructured meshes., Proc. 27th AIAA Aerospace Sciences Meeting.
- Bayley, F. J. and Owen, J. 1970. The fluid dynamics of a shrouded disk system with a radial outflow of coolant; ASME J. Eng. Power, v. 92, pp 335-341
- Graber, D. J., Daniels, W. A. and Johnson, B. V. 1987. Disk pumping test, Final Report. Air Force Wright Aeronautical Laboratories, Report No. AFWAL-TR-87- 2050
- Jarzombek, K, Benra, F.-K., H. Dohmen, J. and Schneider, O., 2007. CFD analysis of flow in high-radius pre-swirl systems, ASME paper GT2007-27404
- Lewis, P., Wilson, M., Lock, G. D., and Owen, J., 2007. Physical interpretation of flow and heat transfer in pre-swirl systems, J. Engineering for Gas Turbines and Power, v. 129, n. 3, pp 769-777
- Lock, G. D., Wilson, M. and Owen, J. M., 2005. Heat transfer measurements using liquid crystals in a pre-swirl rotating-disc system, J. Engineering for Gas Turbines and Power , v. 127, n. 2, pp 375-382
- Menter, F. R., 1994. "Two-equation eddy viscosity turbulence models for engineering applications". AIAA-Journal, 8(32), pp. 269-289.
- Owen, J. M., 2006. Modelling internal air systems in gas turbine engines, Proc. 1st Int. Symp. Jet Propulsion & Power Eng., Kunming, China, Sept 17-22
- Owen, J. M., and Rogers, R. H., 1989, Flow and heat transfer in rotating disc systems: Vol. 1, Rotor-Stator Systems, Research Studies Press, Taunton, UK and Wiley, New York.
- Phadke, U.P. and Owen, J.M. 1988a. Aerodynamic aspects of the sealing of gas-turbine rotor-stator systems, Part 1: The behaviour of simple shrouded rotating-disk systems in a quiescent environment, Int J Heat Fluid Flow, v. 9, pp 98-105
- Phadke, U.P. and Owen, J.M. 1988b. Aerodynamic aspects of the sealing of gas-turbine rotor-stator systems, Part 2: The performance of simple seals an a quasi-axisymmetric external flow, Int J Heat Fluid Flow, v. 9, pp 106-112
- Phadke, U.P. and Owen, J.M. 1988c. Aerodynamic aspects of the sealing of gas-turbine rotor-stator systems, Part 3: The effect of non-axisymmetric external flow on seal performance, Int J Heat Fluid Flow, v. 9, pp 113-117
- Rhie, C. M., and Chow, W. L., 1982. "A numerical study of the turbulent flow past an isolated airfoil with trailing edge separation". AIAA Paper 82-0998.
- Roy, R. P., Zhou, D. W., Ganesan, S., Wang, C-Z, Paolillo, R. E. and Johnson, B. V., 2007. The flow field and main gas ingestion in a rotor-stator cavity, ASME paper GT2007-27671
- Sun, Z, Lindblad, K, Chew, J. W. and Young, C, 2006. LES and

RANS investigations into buoyancy affected convection in a rotating cavity with a central axial throughflow, J. Engineering for Gas Turbines and Power, v. 129, n. 3, pp.318-325

Wang, C-Z, Johnson, B. V., De Jong, F. and Vashist, T. K., 2007. Comparison of flow characteristics in axial gap seals for close and wide-spaced turbine stages, ASME paper GT2007-27909